

Site-selective NMR for odd-frequency Cooper pairs around vortex in chiral p -wave superconductors

Kenta K. Tanaka,* Masanori Ichioka,[†] and Seiichiro Onari

Department of Physics, Okayama University, Okayama 700-8530, JAPAN

(Dated: March 3, 2016)

In order to identify the pairing symmetry with chirality, we study site-selective NMR in chiral p -wave superconductors. We calculate local nuclear relaxation rate T_1^{-1} in the vortex lattice state by Eilenberger theory, including the applied magnetic field dependence. We find that T_1^{-1} in the NMR resonance line shape is different between two chiral states $p_{\pm}(=p_x \pm ip_y)$, depending on whether the chirality is parallel or anti-parallel to the vorticity. Anomalous suppression of T_1^{-1} occurs around the vortex core in the chiral p_- -wave due to the negative coherence term coming from the odd-frequency s -wave Cooper pair induced around the vortex with Majorana state.

PACS numbers: 74.20.Rp, 74.25.Uv, 74.25.nj, 74.25.Ha

I. INTRODUCTION

In the study of unconventional superconductors, it is most important to identify the spin and orbital symmetry of the Cooper pairs since it is tightly related to the mechanism of superconductivity. The pairing symmetry of the ruthenate superconductor Sr_2RuO_4 is suggested to be chiral p_{\pm} -wave^{1,2}, where Cooper pairs have angular momentum $L_z = \pm 1$ for $p_{\pm} = p_x \pm ip_y$. For experimental evidence, the spin triplet pairing is supported by the Knight shift measurement³ and the broken time-reversal symmetry coming from the chiral pair was observed by μSR ⁴ and polar Kerr effect⁵ measurements. However, any experiment to identify the direction of the chirality, i.e., p_+ or p_- in Sr_2RuO_4 is not yet realized, since the μSR and the polar Kerr effect measurements can only detect the existence of chirality ($L_z = 0$ or $\neq 0$).

The spatially resolved NMR measurement⁶⁻⁹ called site-selective NMR can detect local electronic states related to the pairing symmetry in the vortex lattice state by selectively observing the resonance field dependence of the nuclear relaxation rate T_1^{-1} in the NMR resonance line shape. This measurement is complementary method to the scanning tunneling microscopy measurement, since the NMR measurement is free from the material surface condition. From our previous studies for site-selective NMR^{10,11}, local $(T_1 T)^{-1}$ in the vortex lattice state is determined by local density of states (DOS) of electrons in the s - and $d_{x^2-y^2}$ -wave superconductors. As for the chiral p -wave superconductor, previous theories suggest that the temperature T -dependence of T_1^{-1} is different between p_+ and p_- states at the vortex center¹²⁻¹⁴. This chirality-dependence is caused by the interaction between the chirality and vorticity, depending on whether the chirality $L_z(= \pm 1)$ is parallel or anti-parallel to the vorticity $W(= 1)$ in the vortex state of chiral p -wave superconductors¹⁵⁻¹⁸.

Recently, the chiral p -wave superconductors have been attracting much attention as a topological superconductor, since it has non-trivial topological properties. In this superconductor, topological defects such as vortex or sur-

face induce Majorana fermions¹⁹⁻²¹. Majorana fermions give rise to anomalous electric states such as Majorana zero mode and non-Abelian statistics of the vortices²⁰. In addition, the vortex state of chiral p -wave superconductors also induces odd-frequency Cooper pairs^{18,22,23}. In particular, the odd-frequency s -wave Cooper pair in the vortex state of chiral p -wave superconductors is related to the Majorana fermion²³.

The purpose of this paper is that we investigate the method to identify the pairing symmetry with chirality by the site-selective NMR measurement. In chiral p -wave superconductors, it is significant to prove topological numbers L_z and W as well as local DOS. From this view point, we study the chirality-dependence of local $T_1^{-1}(\mathbf{r})$ in the resonance field dependence in the vortex lattice state. We especially focus on anomalous suppression of T_1^{-1} around the vortex core in the chiral p_- -wave. Further, we will discuss reasons for the anomalous suppression of T_1^{-1} in the relation to odd-frequency Cooper pairs induced around the vortex with Majorana state.

This paper is organized as follows. After the introduction, we explain our formulation of Eilenberger theory for the vortex lattice state, and calculation method for T_1^{-1} in Sec. II. In Sec. III, we study the temperature, spatial and resonance field dependence of local $T_1^{-1}(\mathbf{r})$ in the vortex lattice state. In Sec. IV, we discuss the reasons for the anomalous suppression of T_1^{-1} . The last section is devoted to summary.

II. FORMULATION

We calculate the spatial structure of the vortex lattice state by quasiclassical Eilenberger theory^{11,16,24}. The quasiclassical theory is valid when the atomic scale is enough small compared to the superconducting coherence length ξ . For many superconductors including Sr_2RuO_4 , this quasiclassical condition is well satisfied^{1,2}. Moreover, since our calculations are performed in the vortex lattice state, distributions of local T_1^{-1} and the resonance field are quantitatively obtained as a function of temperature and applied field. Therefore, our calcu-

lation method is powerful and reliable tool dealing with the inhomogeneous spatial structure of superconducting properties.

As a simple model of Sr_2RuO_4 , we consider the chiral p -wave pairing on the cylindrical Fermi surface, $\mathbf{k} = (k_x, k_y) = k_F(\cos \theta_k, \sin \theta_k)$, and the Fermi velocity $\mathbf{v}_F = v_{F0}\mathbf{k}/k_F$. Quasiclassical Green's functions $g(i\omega_n, \mathbf{k}, \mathbf{r})$, $f(i\omega_n, \mathbf{k}, \mathbf{r})$, $f^\dagger(i\omega_n, \mathbf{k}, \mathbf{r})$ are calculated by solving Eilenberger equation

$$\begin{aligned} \{\omega_n + \mathbf{v} \cdot (\nabla + i\mathbf{A}(\mathbf{r}))\} f &= \tilde{\Delta}(\mathbf{r}, \mathbf{k})g, \\ \{\omega_n - \mathbf{v} \cdot (\nabla - i\mathbf{A}(\mathbf{r}))\} f^\dagger &= \tilde{\Delta}^*(\mathbf{r}, \mathbf{k})g, \end{aligned} \quad (1)$$

where $g = (1 - f f^\dagger)^{1/2}$, and $\mathbf{v} = \mathbf{v}_F/v_{F0}$. The order parameter is $\tilde{\Delta}(\mathbf{r}, \mathbf{k}) = \Delta_+(\mathbf{r})\phi_{p+}(\mathbf{k}) + \Delta_-(\mathbf{r})\phi_{p-}(\mathbf{k})$ with the pairing function $\phi_{p\pm}(\mathbf{k}) = (k_x \pm ik_y)/k_F = e^{\pm i\theta_k}$ for the chiral p_{\pm} -wave. \mathbf{r} is the center-of-mass coordinate of the pair. When magnetic fields are applied along the z axis, the vector potential is given by $\mathbf{A}(\mathbf{r}) = \frac{1}{2}\mathbf{H} \times \mathbf{r} + \mathbf{a}(\mathbf{r})$ in the symmetric gauge, where $\mathbf{H} = (0, 0, H)$ is a uniform flux density, and $\mathbf{a}(\mathbf{r})$ is related to the internal field $\mathbf{B}(\mathbf{r}) = (0, 0, B(\mathbf{r})) = \mathbf{H} + \nabla \times \mathbf{a}(\mathbf{r})$. We have scaled temperature, length, and magnetic field in unit of T_{c0} , ξ_0 , and B_0 , where $\xi_0 = \hbar v_{F0}/2\pi k_B T_{c0}$, $B_0 = \phi_0/2\pi \xi_0^2$ with the flux quantum ϕ_0 , respectively. T_{c0} is transition temperature at a zero field. The energy E , pair potential Δ and Matsubara frequency ω_n are in unit of $\pi k_B T_{c0}$. In the following, we set $\hbar = k_B = 1$.

To determine $\Delta_{\pm}(\mathbf{r})$ and the quasiclassical Green's functions selfconsistently, we calculate $\Delta_{\pm}(\mathbf{r})$ by the gap equation

$$\Delta_{\pm}(\mathbf{r}) = g_0 N_0 T \sum_{0 < \omega_n \leq \omega_{\text{cut}}} \left\langle \phi_{p\pm}^*(\mathbf{k}) \left(f + f^\dagger \right) \right\rangle_{\mathbf{k}}, \quad (2)$$

where $(g_0 N_0)^{-1} = \ln T + 2T \sum_{0 < \omega_n \leq \omega_{\text{cut}}} \omega_n^{-1}$, and we use $\omega_{\text{cut}} = 20k_B T_{c0}$. $\langle \cdots \rangle_{\mathbf{k}}$ indicates the Fermi surface average. For the selfconsistent calculation of the vector potential for the internal field $B(\mathbf{r})$, we use the relation

$$\nabla \times (\nabla \times \mathbf{A}) = -2T\kappa^{-2} \sum_{0 < \omega_n} \langle \mathbf{v} \text{Im}\{g\} \rangle_{\mathbf{k}}. \quad (3)$$

In our calculations, we use the Ginzburg-Landau parameter^{11,24,25} $\kappa = 2.7$ appropriate to Sr_2RuO_4 ^{1,2}.

We iterate calculations of Eqs. (1)-(3) in Matsubara frequency ω_n in the square vortex lattice²⁶, until we obtain the selfconsistent results of $\mathbf{A}(\mathbf{r})$, $\Delta(\mathbf{r})$ and the quasiclassical Green's functions. We consider two states of p_{\pm} . In the p_+ state, where chirality and vorticity are parallel, $\Delta_+(\mathbf{r})$ is main component and $\Delta_-(\mathbf{r})$ is induced around vortices. In the p_- state where $\Delta_-(\mathbf{r})$ is main component, chirality and vorticity are anti-parallel. The studies of phase diagram for thermodynamically stable states have been already reported in Refs.^{15,16}. According to these previous studies, the p_- state has a lower free energy than the metastable p_+ state in all T - H range except for $H = 0$. At the $H = 0$, the chiral p_{\pm} states are degenerate in free energy. We study not only the stable p_- state case but also the metastable p_+ state case.

From our calculation results, the upper critical field is $H_{c2}/B_0 = 0.84$ at $T/T_{c0} = 0.5$ for the p_- state. The p_+ state is unstable at $H/B_0 > 0.31$ at $T/T_{c0} = 0.5$, and changes to the p_- state.

Next, using the selfconsistently obtained $\mathbf{A}(\mathbf{r})$ and $\Delta(\mathbf{r})$, we calculate quasiclassical Green's functions in real energy $E \pm i\eta$ instead of $i\omega_n$. Since we consider the clean case with long lifetime of quasiparticle, we use enough small $\eta (= 0.01)$, maintaining the accuracy of numerical calculation. We solve Eilenberger equation (1) with $i\omega_n \rightarrow E \pm i\eta$ to obtain $g(E \pm i\eta, \mathbf{k}, \mathbf{r})$, $f(E \pm i\eta, \mathbf{k}, \mathbf{r})$, $f^\dagger(E \pm i\eta, \mathbf{k}, \mathbf{r})$. The local DOS $N(E, \mathbf{r})$ is given by $N(E, \mathbf{r}) = \langle \text{Re}\{g(E \pm i\eta, \mathbf{k}, \mathbf{r})\} \rangle_{\mathbf{k}}$.

Based on the linear response theory, from the obtained quasiclassical Green's functions, the nuclear relaxation rate T_1^{-1} is calculated as^{11,13}

$$\begin{aligned} \frac{(T_1(T)T)^{-1}}{(T_1(T_c)T_c)^{-1}} &= \frac{(T_{1gg}(T)T)^{-1} + (T_{1ff}(T)T)^{-1}}{(T_1(T_c)T_c)^{-1}} \\ &= \int_{-\infty}^{\infty} \frac{W_{gg}(E, \mathbf{r}) + W_{ff}(E, \mathbf{r})}{4T \cosh^2(E/2T)} dE, \end{aligned} \quad (4)$$

where

$$\begin{aligned} W_{gg}(E, \mathbf{r}) &= \langle a_{\downarrow\downarrow}^{22}(E, \mathbf{k}, \mathbf{r}) \rangle_{\mathbf{k}} \langle a_{\uparrow\uparrow}^{11}(-E, \mathbf{k}, \mathbf{r}) \rangle_{\mathbf{k}}, \\ W_{ff}(E, \mathbf{r}) &= -\langle a_{\downarrow\uparrow}^{21}(E, \mathbf{k}, \mathbf{r}) \rangle_{\mathbf{k}} \langle a_{\uparrow\downarrow}^{12}(-E, \mathbf{k}, \mathbf{r}) \rangle_{\mathbf{k}} \end{aligned} \quad (5)$$

with

$$\begin{aligned} a_{\uparrow\uparrow}^{11}(E, \mathbf{k}, \mathbf{r}) &= \frac{1}{2} [g(E + i\eta, \mathbf{k}, \mathbf{r}) - g(E - i\eta, \mathbf{k}, \mathbf{r})], \\ a_{\downarrow\downarrow}^{22}(E, \mathbf{k}, \mathbf{r}) &= \frac{1}{2} [\bar{g}(E + i\eta, \mathbf{k}, \mathbf{r}) - \bar{g}(E - i\eta, \mathbf{k}, \mathbf{r})], \\ a_{\downarrow\downarrow}^{12}(E, \mathbf{k}, \mathbf{r}) &= \frac{i}{2} [f(E + i\eta, \mathbf{k}, \mathbf{r}) - f(E - i\eta, \mathbf{k}, \mathbf{r})], \\ a_{\downarrow\uparrow}^{21}(E, \mathbf{k}, \mathbf{r}) &= \frac{i}{2} [f^\dagger(E + i\eta, \mathbf{k}, \mathbf{r}) - f^\dagger(E - i\eta, \mathbf{k}, \mathbf{r})] \end{aligned} \quad (6)$$

and $\bar{g}(E, \mathbf{k}, \mathbf{r}) = g(E, \mathbf{k}, \mathbf{r})$. $T_c (< T_{c0})$ is superconducting transition temperature at a finite magnetic field. We define $t = T/T_c$. $(T_{1gg}T)^{-1}$ is the contribution in $(T_1T)^{-1}$ from the DOS term W_{gg} , and $(T_{1ff}T)^{-1}$ is the contribution from the coherence term W_{ff} .

III. LOCAL NMR RELAXATION RATE

First, we study the T -dependence of local $(T_1T)^{-1}$ shown in Fig. 1 for p_{\pm} states. For a reference, we also show the $d_{x^2-y^2}$ -wave pairing state $\tilde{\Delta}(\mathbf{r}, \mathbf{k}) = \Delta_d(\mathbf{r})\sqrt{2}\cos 2\theta_k$ ¹¹. Outside of vortex core, such as the midpoint between next nearest neighbor (NNN) vortices in Fig. 1(a), the T -dependence is similar to the bulk chiral p -wave superconductors in both p_{\pm} states. There, we see exponential T -dependence at low T , reflecting the full gap $|\phi_{p\pm}| = 1$. On the other hand, around the vortex core in Figs. 1(b) and 1(c), we see the different behaviors depending on the chirality directions. In the p_+ state, $(T_1T)^{-1}$ is more enhanced with approaching the

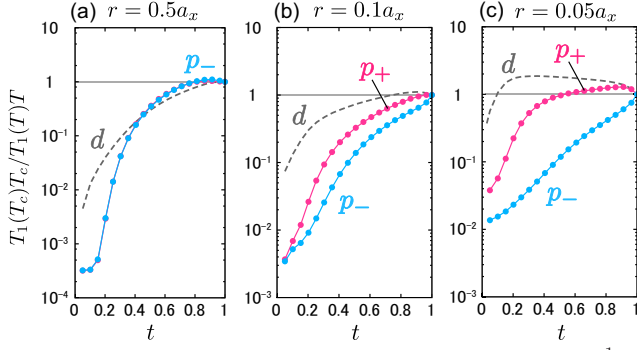


FIG. 1. (Color online) T -dependence of local $(T_1T)^{-1}$ for the p_{\pm} states at radius $r/a_x = 0.5$ (a), 0.1 (b), 0.05 (c) from the vortex center along the NNN vortex direction. a_x is inter vortex distance along the NNN direction. We plot normalized values $(T_1(T)T)^{-1}/(T_1(T_c)T_c)^{-1}$ as a function of t at $H/B_0 = 0.02$. The vertical axis is a logarithmic scale. The $d_{x^2-y^2}$ -wave case is also shown for reference. $T_c/T_{c0} = 0.985$ (0.975) at $H/B_0 = 0.02$ in the p_{\pm} ($d_{x^2-y^2}$) states.

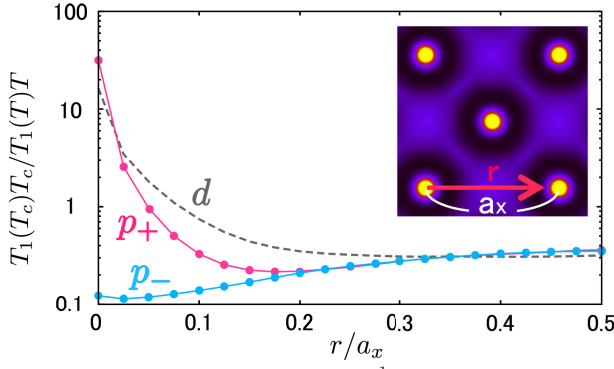


FIG. 2. (Color online) Local $(T_1T)^{-1}$ as a function of radius r/a_x from the vortex center along the NNN direction for the p_+ and p_- states. The $d_{x^2-y^2}$ -wave case is also shown. The vertical axis is a logarithmic scale. $T/T_{c0} = 0.5$ and $H/B_0 = 0.02$. $(T_1T)^{-1}$ is normalized by the value at T_c . The inset shows a spatial structure of $(T_1T)^{-1}$ for the p_+ state. Brighter region has larger $(T_1T)^{-1}$.

vortex center. This enhancement is due to the localized low energy DOS around the vortex core, and moderate compared to the $d_{x^2-y^2}$ -wave pairing state¹¹. However, the enhancement does not occur in the p_- state in Figs. 1(b) and 1(c). The reason of this suppression is related to the odd-frequency Cooper pairs around the vortex core, as discussed later.

As shown in Fig. 2, to see the spatial dependence in detail, we present local $(T_1T)^{-1}$ as a function of radius r on a line between NNN vortices. Outside of the vortex core $r/a_x \geq 0.2$, $(T_1T)^{-1}$ shows almost the same r -dependence between the p_+ and p_- states. Inside the vortex core, it is characteristic that $(T_1T)^{-1}$ is enhanced in the p_+ state, but it is anomalously suppressed in the p_- state. It is also noted that $(T_1T)^{-1}$ monotonically decreases as a function of r in the d -wave, but it has a minimum at $r \sim 0.175a_x$ in the p_+ state. The minimum region surrounding the vortex core is also seen in

the spatial structure of $(T_1(\mathbf{r})T)^{-1}$ shown in the inset of Fig. 2.

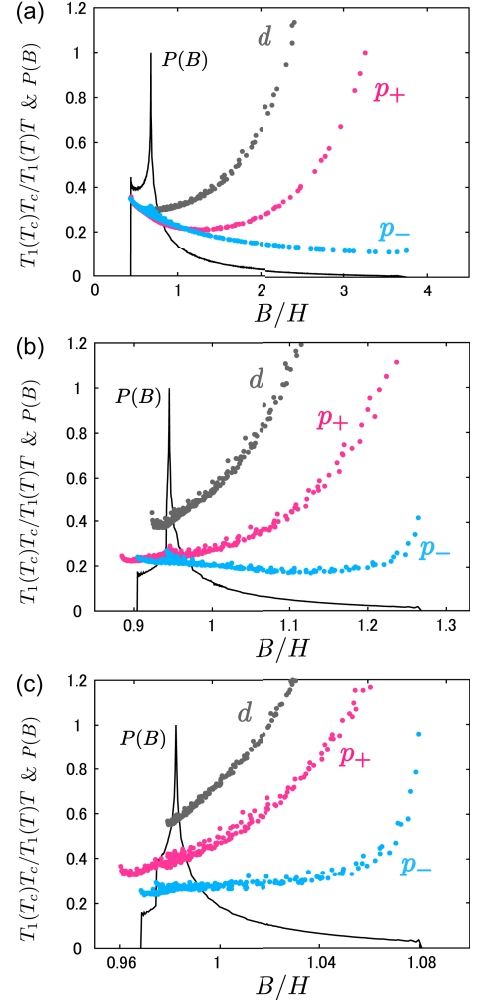


FIG. 3. (Color online) Solid lines indicate the Redfield pattern of the NMR resonance line shape, $P(B)$, for the p_- state. Points are for B -dependence of $(T_1T)^{-1}$ for the p_+ and p_- states. The $d_{x^2-y^2}$ -wave case is also shown. $T/T_{c0} = 0.5$ and $H/B_0 = 0.02$ (a), 0.10 (b), 0.20 (c). $(T_1T)^{-1}$ is normalized by the value at T_c . Only data points $(T_1T)^{-1} \leq 1.2$ are presented in (a), (b) and (c).

Next, we discuss how the difference between p_+ and p_- states is detected in the site-selective NMR measurement. From the internal field distribution $\mathbf{B}(\mathbf{r})$, we theoretically obtain the Redfield pattern²⁷ of the NMR resonance line shape, as $P(\omega) = \int \delta(\omega - B(\mathbf{r}))d\mathbf{r}$, since the intensity at each resonance frequency ω comes from the volume satisfying $\omega = B(\mathbf{r})$ in a unit cell. In Sr_2RuO_4 , $P(B)$ was observed by μSR ²⁸. In Fig. 3(a), with $P(B)$, we plot local $(T_1T)^{-1}$ as a function of local field $B(\mathbf{r})$ at the same position \mathbf{r} . At lower resonance fields $B/H < 1$ near the peak of $P(B)$, NMR signals come from outside of the vortex cores. In this range, $(T_1T)^{-1}$ decreases as a function of B in both p_{\pm} states similarly. The tail of $P(B)$ at higher B is approaching the vortex center. In this range $B/H > 1$, we can see the chirality dependence,

Symmetry component	Chirality L_z	Vorticity W	
		p_+ state	p_- state
d_{2+}	2	0 (center)	-2
p_+	1	1 (main)	-1
s	0	2	0 (center)
p_-	-1	3	1 (main)
d_{2-}	-2	4	2
		$L_z + W = 2$	$L_z + W = 0$

TABLE I. Relation of vorticity W and chirality L_z for each symmetry component of the orbital-decomposed Cooper pair \mathcal{F}_m around a vortex in the p_+ and p_- states. Main component in each case has $W = 1$. The induced component has other W locally around the vortex center by the conservation of $L_z + W$ ¹⁸. At the vortex center, induced component with $W = 0$ has finite amplitude.

i.e., $(T_1 T)^{-1}$ increases as a function of B in the p_+ state, but it decreases in the p_- state. However, at the low applied field H , the signal of the vortex core contribution at higher B is weak in $P(B)$. On the other hand, at higher applied field H as shown in Figs. 3(b) and 3(c), the signal for distinguishing the chirality becomes larger in $P(B)$, since weight of the vortex core region increases within the unit cell of the vortex lattice with increasing H . In Fig. 3(b), $(T_1 T)^{-1}$ in the p_+ state increases as a function of B in all resonance field range, while it is almost flat in the p_- state except for largest B . In Fig. 3(c), $(T_1 T)^{-1}$ in both p_{\pm} states increases as a function of B . From these calculation results, we can identify the direction of the chirality i.e., p_+ or p_- state by measuring B -dependence of $(T_1 T)^{-1}$. In particular, it is important that we observe the monotonically decreasing or flat behavior of $(T_1 T)^{-1}$ as a function of B , since this behavior is realized only in the p_- state. And, from the previous studies^{15,16}, it is expected that the p_- state has a lower free energy than the metastable p_+ state in the vortex state. However, we should be careful about strength of applied field, since B -dependence of $(T_1 T)^{-1}$ changes as shown in Fig. 3(c), when the applied field is too high.

IV. RELATION TO ODD-FREQUENCY COOPER PAIRS

To discuss the reasons for the anomalous suppression of T_1^{-1} around the vortex core in the chiral p -wave superconductors, we present the decomposition of $(T_1 T)^{-1}$ to the DOS term $(T_{1gg} T)^{-1}$ and the coherence term $(T_{1ff} T)^{-1}$ in Figs. 4(a) and 4(b). There, we see that $(T_{1gg} T)^{-1}$ is enhanced around the vortex core in both p_{\pm} states similarly, as in the s - and $d_{x^2-y^2}$ -wave cases¹¹. The enhancement reflects low energy DOS around the vortex core. The chirality-dependence appears in negative coherence term $(T_{1ff} T)^{-1}$. In the p_- state, negative $(T_{1ff} T)^{-1}$ cancels the enhancement of $(T_{1gg} T)^{-1}$, so that $(T_1 T)^{-1}$ is suppressed in the vortex core. In the p_+ state, weak suppression of $(T_1 T)^{-1}$ in the region surrounding vortex in

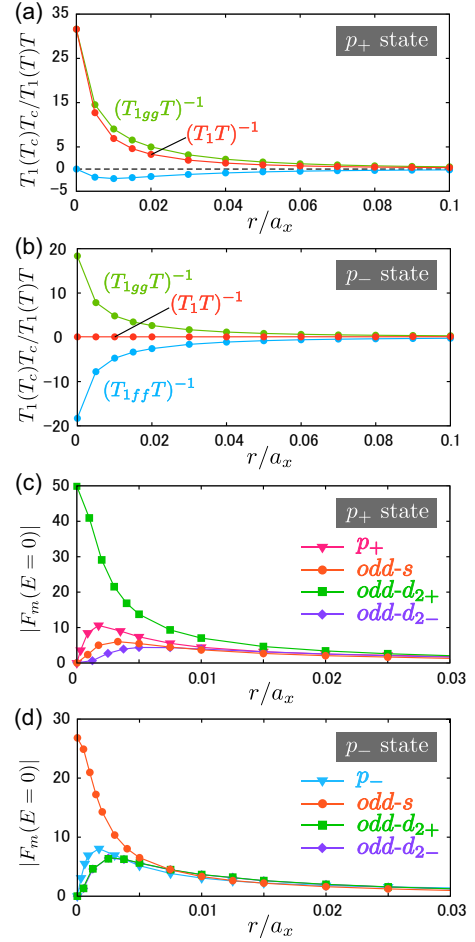


FIG. 4. (Color online) r -dependence of $(T_1 T)^{-1}$, $(T_{1gg} T)^{-1}$, $(T_{1ff} T)^{-1}$ in (a) the p_+ state and (b) the p_- state. $(T_1 T)^{-1}$, $(T_{1gg} T)^{-1}$, $(T_{1ff} T)^{-1}$ is normalized by $(T_1(T_c)T_c)^{-1}$. r -dependence of orbital-decomposed Cooper pair's amplitude $|\mathcal{F}_m(E=0)|$ in (c) the p_+ state and (d) the p_- state. $m = s, p_{\pm}$, and $d_{2\pm}$. In all figures, $T/T_{c0} = 0.5$ and $H/B_0 = 0.02$. r is radius from the vortex center along the NNN vortex direction. In the p_- state, $|\mathcal{F}_{d_{2+}}(r, E=0)| \sim |\mathcal{F}_{d_{2-}}(r, E=0)|$.

Fig. 2 is also due to the small negative term $(T_{1ff} T)^{-1}$. Therefore, in the p_+ state, we can say that the $(T_{1gg} T)^{-1}$ of a normal signal obscures the $(T_{1ff} T)^{-1}$ of a superfluid response. However, in the p_- state, since the superfluid response is enhanced around the vortex core including the proximity effect of superconductivity, the normal signal does not obscure the superfluid response.

At last, we discuss origin of the negative coherence term. From Eqs. (4)-(6), s -wave pair can contribute to the coherence term $(T_{1ff} T)^{-1}$ since the condition $\langle f \rangle_{\mathbf{k}} \neq 0$ with $L_z = 0$. Actually, in conventional s -wave superconductor, a Hebel-Slichter peak appears below T_c due to the coherence term^{11,29,30}. To check this condition, we calculate orbital-decomposed Cooper pair $\mathcal{F}_m(E, \mathbf{r}) = \langle \phi_m^*(\mathbf{k}) f(E + i\eta, \mathbf{k}, \mathbf{r}) \rangle_{\mathbf{k}}$. In addition to $\phi_{p_{\pm}}(\mathbf{k})$, we employ $\phi_s(\mathbf{k}) = 1$ for the s -wave, and $\phi_{d_{2\pm}}(\mathbf{k}) = e^{\pm i2\theta}$ for the chiral d -wave. The obtained s - and d -wave components in the chiral p -wave superconductors are odd-

frequency Cooper pair¹⁸. In Figs. 4(c) and 4(d), we present the r -dependence of $|\mathcal{F}_m(E=0, \mathbf{r})|$, where the induced s - and d -wave amplitude have large values around the vortex core. As summarized in Table I, the vorticity W of the symmetry component \mathcal{F}_m with the chirality L_z is determined by the condition $L_z + W = 2$ in the p_+ state and $L_z + W = 0$ in the p_- state. In the p_+ state, chiral d_{2+} -wave component has $W = 0$, giving large amplitude at the vortex center. Small induced s -wave component also appears, but it vanishes at the vortex center since it has $W = 2$, as shown in Fig. 4(c). In the p_- state, the s -wave component has $W = 0$ thus it has large amplitude at the vortex center, as shown in Fig. 4(d). The odd-frequency s -wave Cooper pair determines the r -dependence of the negative coherence term $(T_{1ff}T)^{-1}$ in Figs. 4(a) and 4(b). In particular, at low T limit, we confirmed that $(T_{1ff}T)^{-1} \sim -|\mathcal{F}_s(E=0)|^2$ at the vortex center from the calculation results.

The previous theoretical study using the Andreev bound state model showed that T_1^{-1} at the vortex center is completely zero ($T_1^{-1} \sim 0$) due to the coherence effect when the L_z is anti-parallel to the W ¹⁴. On the other hand, previous our study using the Bogoliubov-de Gennes theory confirmed the relation $N(E=0, \mathbf{r}) \propto |\mathcal{F}_s(E=0, \mathbf{r})|$ in the p_- state for the vortex core quasiparticle states with Majorana zero mode²³. Considering these relation, we find that the $(T_{1ff}T)^{-1}$ related to the odd-frequency s -wave Cooper pair tends to cancel the local DOS term $(T_{1gg}T)^{-1}$, since $(T_{1gg}(\mathbf{r})T)^{-1} \sim N(E=0, \mathbf{r})^2$ and $(T_{1ff}(\mathbf{r})T)^{-1} \sim -|\mathcal{F}_s(E=0, \mathbf{r})|^2$ at low T and H limit (low energy limit). Therefore, the anomalous suppression of $(T_1T)^{-1}$ is also explained by the nature of Majorana state. Note that, in our calculation results at finite T and H states, $(T_1T)^{-1}$ is not completely zero around the vortex core, since quasiparticle states different from Majorana zero mode also contribute to the NMR relaxation, as shown in Fig. 2.

When we discuss the influence of the sub-dominant components, we have to distinguish the order parameter Δ and the pair amplitude \mathcal{F} . The sub-dominant components such as odd-frequency s - and d -wave Cooper pairs vanish in the order parameter, since the order parameter is determined by the gap equation of Eq. (2). Therefore, the qualitatively unique mechanism of negative coherence term related to the odd-frequency Cooper pairs in the chiral p -wave superconductors does not seriously depend on the details of setting the pairing interaction for the sub-dominant order parameter.

V. SUMMARY

We have calculated the T -, r - and B -dependence of the local NMR relaxation rate $(T_1T)^{-1}$ in two chiral p_{\pm} states, and $d_{x^2-y^2}$ -wave as a reference. We have clarified that $(T_1T)^{-1}$ in the p_+ state is enhanced with approaching the vortex center by the contribution of low energy excitations of the vortex core, but it is anomalously suppressed around the vortex core in the p_- state. This chirality-dependence of local $(T_1T)^{-1}$ may be observed by the site-selective NMR measurement via the B -dependence of $(T_1T)^{-1}$ in $P(B)$. Further, we have theoretically found that the anomalous suppression of $(T_1T)^{-1}$ around the vortex core is due to the negative coherence term by the induced odd-frequency s -wave Cooper pair with Majorana state.

We hope that these theoretical estimates of local $(T_1T)^{-1}$ will be confirmed by the site-selective NMR measurement, and will be used for detecting the pairing symmetry with chirality in the chiral p -wave superconductors, and natures of odd-frequency Cooper pairs and Majorana states.

* ktanaka@mp.okayama-u.ac.jp

† ichioka@cc.okayama-u.ac.jp

¹ A. P. Mackenzie and Y. Maeno, Rev. Mod. Phys. **75**, 657 (2003).

² Y. Maeno, S. Kittaka, T. Nomura, S. Yonezawa, and K. Ishida, J. Phys. Soc. Jpn. **81**, 011009 (2012).

³ K. Ishida, H. Mukuda, Y. Kitaoka, K. Asayama, Z. Q. Mao, Y. Mori, and Y. Maeno, Nature **396**, 658 (1998).

⁴ G. M. Luke, Y. Fudamoto, K. M. Kojima, M. I. Larkin, J. Merrin, B. Nachumi, Y. J. Uemura, Y. Maeno, Z. Q. Mao, Y. Mori, H. Nakamura, and M. Sigrist, Nature **394**, 558 (1998).

⁵ J. Xia, Y. Maeno, P. T. Beyersdorf, M. M. Fejer, and A. Kapitulnik, Phys. Rev. Lett. **97**, 167002 (2006).

⁶ N. J. Curro, C. Milling, J. Haase, and C. P. Slichter, Phys. Rev. B **62**, 3473 (2000).

⁷ V. F. Mitrović, E. E. Sigmund, M. Eschrig, H. N. Bachman, W. P. Halperin, A. P. Reyes, P. Kuhns, and W. G. Moulton, Nature(London) **413**, 501 (2001).

⁸ K. Kakuyanagi, K.-ichi Kumagai, and Y. Matsuda, Phys. Rev. B **65**, 060503(R) (2002); K. Kakuyanagi, K. Kumagai, Y. Matsuda, and M. Hasegawa, Phys. Rev. Lett. **90**, 197003 (2003).

⁹ Y. Nakai, Y. Hayashi, K. Kitagawa, K. Ishida, H. Sugawara, D. Kikuchi, and H. Sato, J. Phys. Soc. Jpn. **77**, 333 (2008); Y. Nakai, Y. Hayashi, K. Ishida, H. Sugawara, D. Kikuchi, and H. Sato, Physica B **403**, 1109 (2008).

¹⁰ M. Takigawa, M. Ichioka, and K. Machida, Phys. Rev. Lett. **83**, 3057 (1999); J. Phys. Soc. Jpn. **69**, 3943 (2000).

¹¹ K. K. Tanaka, M. Ichioka, S. Onari, N. Nakai, and K. Machida, Phys. Rev. B **91**, 014509 (2015).

¹² M. Takigawa, M. Ichioka, K. Machida, and M. Sigrist, J. Phys. Chem. Solids **63**, 1333 (2002).

¹³ N. Hayashi and Y. Kato, Physica C **388**, 513 (2003); N. Hayashi and Y. Kato, J. Low Temp. Phys. **131**, 893 (2003).

¹⁴ Y. Kato and N. Hayashi, Physica C **388**, 519 (2003).

¹⁵ R. Heeb and D. F. Agterberg, Phys. Rev. B **59**, 7076 (1999).

- ¹⁶ M. Ichioka and K. Machida, Phys. Rev. B **65**, 224517 (2002).
- ¹⁷ M. Ichioka, Y. Matsunaga, and K. Machida, Phys. Rev. B **71**, 172510 (2005).
- ¹⁸ Y. Tanuma, N. Hayashi, Y. Tanaka, and A. A. Golubov, Phys. Rev. Lett **102**, 117003 (2009).
- ¹⁹ N. Read and D. Green, Phys. Rev. B **61**, 10267 (2000).
- ²⁰ D. A. Ivanov, Phys. Rev. Lett. **86**, 268 (2001).
- ²¹ T. Mizushima, M. Ichioka, and K. Machida, Phys. Rev. Lett. **101**, 150409 (2008).
- ²² Y. Tanaka, M. Sato, and N. Nagaosa J. Phys. Soc. Jpn. **81**, 011013 (2012).
- ²³ T. Daino, M. Ichioka, T. Mizushima, and Y. Tanaka, Phys. Rev. B **86**, 064512 (2012).
- ²⁴ K. K. Tanaka, M. Ichioka, N. Nakai, and K. Machida, Phys. Rev. B **89**, 174504 (2014).
- ²⁵ P. Miranović and K. Machida, Phys. Rev. B **67**, 092506 (2003).
- ²⁶ T. M. Riseman, P. G. Kealey, E. M. Forgan, A. P. Mackenzie, L. M. Galvin, A. W. Tyler, S. L. Lee, C. Ager, D. Mck. Paul, C. M. Aegerter, R. Cubitt, Z. Q. Mao, T. Akima, and Y. Maeno, Nature **396**, 242 (1998); **404**, 629(E) (2000).
- ²⁷ W. Fite, II, and A. G. Redfield, Phys. Rev. Lett **17**, 381 (1966).
- ²⁸ C. M. Aegerter, S. H. Lloyd, C. Ager, S. L. Lee, S. Romer, H. Keller, and E. M. Forgan, J. Phys.: Condens. Matter **10**, 7445 (1998).
- ²⁹ L. C. Hebel and C. P. Slichter, Phys. Rev. **113**, 1504 (1959).
- ³⁰ Y. Masuda and A. G. Redfield, Phys. Rev. **125**, 159 (1962).